BMC Cancer

RESEARCH

Open Access

The influence of image selection and segmentation on the extraction of lung cancer imaging radiomics features using 3D-Slicer software

Chunmei Liu[1], Yuzheng He[2] and Jianmin Luo[3*]

Abstract

Purpose Extracting image features can predict the prognosis and treatment effect of non-small cell lung cancer, which has been increasingly confirmed. However, the specific operation using 3D-Slicer still lacks standardization. For example, image segmentation is manually performed based on the lung window or automatically performed through the mediastinal window. The images used for feature extraction are either enhanced or plain scanned. It is questionable whether these influencing factors will affect the extraction results and which results will be affected. This article intends to preliminarily explore the above issues.

Methods This article downloaded images of 22 patients with lung cancer from The Cancer Imaging Archive (TCIA), including 11 cases of adenocarcinoma and 11 cases of squamous cell carcinoma. Perform tumor image segmentation on the lung window and mediastinal window of the plain scan image, and the lung window and mediastinal window of the enhanced image. Manual drawing is used on the lung window, and automatic drawing is used on the mediastinal window and make manual modifications. Extracting radiomics features using Python radiomics. Firstly, analyze the image features of the original sequence and perform the Shapiro test. If it follows a normal distribution, perform an analysis of variance. If it does not follow a normal distribution, perform the Friedman test. Compare the significantly different image features pairwise. Then, a preliminary analysis was conducted on the differences between squamous cell carcinoma and adenocarcinoma in each group.

Results A total of 88 sets of imaging features were extracted, with 107 features in each group. Among them, 33 features showed significant differences. Continuing with pairwise repeated testing, it was found that there were 2 significant differences between enhanced and plain lung windows. There were 12 significant differences between enhanced lung windows and plain mediastinal windows. There is one significant difference between plain scanning and enhancement mediastinal window. There are 14 significant differences between the plain lung window and the enhanced mediastinal window groups. There are 14 significant differences between the lung window and the mediastinal window in the plain scan. There are 13 significant differences between the enhanced lung window and the mediastinal window. According to pathological grouping testing, it was found that there 54 significant differences between squamous cell carcinoma and adenocarcinoma.

*Correspondence:
Jianmin Luo
luojm31555@163.com
Full list of author information is available at the end of the article

Conclusion The enhancement of lung CT has a relatively small impact on extracting image features, while selecting lung or mediastinal windows for image segmentation has a significant impact on extracting image features. Therefore, choosing lung or mediastinal windows for feature extraction should be carefully considered, as the size of the image segmentation range has a significant impact on image features. The impact of lung squamous cell carcinoma and adenocarcinoma on imaging features is also significant, indicating a high possibility of distinguishing between squamous cell carcinoma and adenocarcinoma based on radiomics (Liu C, He Y, Luo J, The Influence of Image Selection and Segmentation on the Extraction of Lung Cancer Imaging Radiomics Features Using 3D-Slicer Software, 2024).

Keywords Lung cancer, 3D-Slicer, Radiomics, Imaging

Introduction

The incidence of lung cancer ranks second among malignant tumors, while the mortality rate ranks first [1]. Traditional diagnostic and treatment methods are no longer sufficient to meet the needs of today's lung cancer patients. In order to improve the quality of life and survival rate of lung cancer patients, better diagnostic and treatment methods, more drugs, and better methods for predicting treatment outcomes are needed. The imaging radiomics technology has enormous potential to assist in the diagnosis and treatment of lung cancer. We can apply radiomics features to differentiate pathology [2–4], gene mutation status [5, 6], predict treatment efficacy [7, 8], recurrence risk [9, 10], survival time [11, 12], and risk of treatment side effects [13, 14]. Of course, the application of these methods is not yet mature and cannot replace traditional methods, but their potential cannot be ignored.

There are more and more studies on radiomics, from diagnosis to treatment selection, and even to prediction of outcomes, the presence of radiomics can be seen. Currently, the most widely used tool for feature extraction in radiomics is 3D Slicer software, as it is free and easy to operate. With continuous updates on new plugins and increasing functionality, it is an important tool for feature extraction in radiomics [15]. However, when using 3D Slicer software for image segmentation, the selected images lack standards. Common images used for lung tumor segmentation include CT and PET-CT. However, Stefano found that the stability of image segmentation using PET-CT was poor [16], so we chose CT images for our research. Through literature review, we found that there is also a lack of standards for CT selection, such as whether CT is enhanced or not, and there is also no uniformity in selecting lung window or mediastinal window for image segmentation. Some studies use non enhanced CT to extract image features [7, 10, 17], some studies use enhanced CT to extract image features [5, 6, 8]. The aim of this experiment is to investigate the impact of these differences on radiomics feature data and to determine the optimal choice with minimal influence. At the same time, the CT scans selected in this study were from patients with adenocarcinoma and squamous cell carcinoma, which account for 70–80% of lung cancer and are representative. Therefore, we can also preliminarily study the differences between lung adenocarcinoma and lung squamous cell carcinoma in different CT groups [18].

Materials and Methods

This article downloads images of 22 lung cancer patients from The Cancer Imaging Archive (TCIA) [19, 20]. Inclusion criteria: 1. Patients diagnosed with lung squamous cell carcinoma or lung adenocarcinoma; 2. The CT scanning range can fully cover the tumor; 3. Clear tumor boundaries; 4. It has both flat scanning and enhanced images. Exclusion criteria: 1. Patients with non squamous cell carcinoma or adenocarcinoma in pathology; 2. The CT scan range cannot fully include the tumor; 3. Tumor boundaries are difficult to determine due to the following reasons: pleural effusion, pneumonia, severe invasion of the hilum of the lungs, severe invasion of the mediastinum or pleura; 4. Lack of enhanced or flat scan images. Import the image into the 3D slicer, and for each patient, only consider the main lesion, which is the total tumor volume (GTV). Adjust the delineation and extraction conditions, and perform 4 segmentation methods for each patient: 1. Plain scan lung window group: Select a lung window on the CT plain scan image and manually delineate GTVf based on the tumor range displayed on the lung window; 2. Enhanced lung window group: Select a lung window on the CT enhanced image and manually delineate GTVfq based on the tumor range displayed on the lung window; 3. Plain scan mediastinal window group: Select the mediastinal window on the CT plain scan image, set the CT domain value to (-150-500hu), and automatically draw GTVz. Draw according to the tumor range of the mediastinal window, and make manual revisions if necessary; 4. Enhanced mediastinal window group: Select the mediastinal window on the CT enhanced image, set the CT domain value to (-150-500hu), and automatically draw GTVzq. Draw according to the tumor range of the mediastinal window and make

manual revisions if necessary. GTVf and GTVz extract image features from CT plain scan images, while GTVfq and GTVzq extract image features from CT enhanced images. 22 patients, each with 4 sets of imaging features, extracted a total of 88 sets of imaging features, each containing 851 features. When using the Python3.7 radiomics function to extract radiomics features from images, all images were preprocessed by resampling voxels into isotropic 1 * 1 * 1. When extracting data features, the following settings were set: binWidth = 25. The characteristics of the patient are shown in Appendix 1. Select a total of 107 features from the original sequence for analysis. First, perform Shapiro test on the four sets of image features. If they conform to a normal distribution, perform analysis of variance. If they are not normally distributed, perform Friedman test. Compare the significantly different image features pairwise. Then, according to the pathology, they are divided into two groups. First, Shapiro test is performed. If the distribution is normal, independent sample T-test is performed. If the distribution is not normal, Wilcoxon rank test is performed.

Results

Lung cancer images of 22 patients, including 11 cases of adenocarcinoma and 11 cases of squamous cell carcinoma. Four sets of influencing features were extracted for each patient, namely the plain lung window group, plain mediastinal window group, enhanced lung window group, and enhanced mediastinal window group. A total of 88 sets of image features were extracted, each containing 851 features. Due to filtering adjustments made to sequences outside the original sequence, the stability cannot be determined. Therefore, a total of 107 features of the original sequence were selected for analysis. Four sets of data for each feature were first subjected to Shapiro tests, all of which were non normal distributions, and Friedman tests were performed. Among them, 33 features showed significant intergroup differences, as shown in Table 1.

Perform the Wilcoxon rank test on 33 features in pairs within the group, with two groups showing significant differences: the plain lung window group and the enhanced lung window group, as shown in Table 2.

There are 12 significant differences between the enhanced lung window and the plain scanning mediastinal window, as shown in Table 3.

There is one significant difference between plain scanning and enhancement of the mediastinal window, as shown in Table 4.

There are 14 significant differences between the plain scan lung window and the enhanced mediastinal window groups, as shown in Table 5.

Table 1 intergroup significant differences

characteristics	group -P
original-shape-LeastAxisLength	1.16438E-08
original-shape-MajorAxisLength	9.26044E-08
original-shape-Maximum2DDiameterColumn	0.0155954
original-shape-Maximum2DDiameterRow	0.0398511
original-shape-Maximum2DDiameterSlice	0.013897644
original-shape-Maximum3DDiameter	0.005388771
original-shape-MeshVolume	0.00028303
original-shape-MinorAxisLength	3.65474E-08
original-shape-SurfaceArea	0.005176663
original-shape-SurfaceVolumeRatio	0.001479286
original-shape-VoxelVolume	0.000269856
original-firstorder-10Percentile	2.30725E-10
original-firstorder-90Percentile	0.003636033
original-firstorder-Energy	1.42605E-10
original-firstorder-Skewness	0.001912288
original-glcm-Idmn	0.002408284
original-glcm-Idn	0.00618336
original-glcm-Imc1	0.000955016
original-gldm-DependenceVariance	0.027875081
original-gldm-LargeDependenceHighGrayLevelEmphasis	0.014577027
original-glrlm-GrayLevelNonUniformity	0.000151633
original-glrlm-LongRunHighGrayLevelEmphasis	0.000682814
original-glrlm-LowGrayLevelRunEmphasis	0.016113473
original-glszm-SmallAreaHighGrayLevelEmphasis	5.16E-08
original-glszm-SmallAreaLowGrayLevelEmphasis	2.47E-07
original-glszm-ZoneEntropy	5.30E-08
original-glszm-ZonePercentage	4.64E-08
original-glszm-ZoneVariance	6.24E-07
original-ngtdm-Busyness	1.26E-05
original-ngtdm-Coarseness	0.040425894
original-ngtdm-Complexity	1.21E-09
original-ngtdm-Contrast	4.83E-09
original-ngtdm-Strength	3.90E-05

Table 2 significant differences between the plain lung window group and the enhanced lung window group

characteristics	P
original-glcm-Imc1	0.021025458
original-ngtdm-Complexity	0.017242836

There are 14 significant differences between the lung window and mediastinal window in plain scan, as shown in Table 6.

Table 3 significant differences between the enhanced lung window and the plain scanning mediastinal window

characteristics	P
original-firstorder-10Percentile	1.62759E-07
original-firstorder-Energy	5.10917E-06
original-firstorder-Skewness	0.019692889
original-glcm-Imc1	0.000194338
original-glszm-SmallAreaHighGrayLevelEmphasis	0.000111445
original-glszm-SmallAreaLowGrayLevelEmphasis	0.000667073
original-glszm-ZoneEntropy	5.10917E-06
original-glszm-ZonePercentage	0.003346064
original-ngtdm-Busyness	0.000808753
original-ngtdm-Complexity	3.37273E-05
original-ngtdm-Contrast	0.000667073
original-ngtdm-Strength	4.88686E-05

Table 4 significant difference between plain scanning and enhancement of the mediastinal window

characteristics	P
original-firstorder-90Percentile	0.036536452

Table 5 significant differences between the plain scan lung window and the enhanced mediastinal window groups

characteristics	P
original-firstorder-10Percentile	6.21914E-06
original-firstorder-Energy	2.42584E-06
original-glcm-Idmn	0.023922019
original-gldm-DependenceVariance	0.007351685
original-glrlm-LowGrayLevelRunEmphasis	0.022434047
original-glszm-SmallAreaHighGrayLevelEmphasis	3.36834E-07
original-glszm-SmallAreaLowGrayLevelEmphasis	4.32389E-05
original-glszm-ZoneEntropy	2.97324E-05
original-glszm-ZonePercentage	7.94135E-07
original-glszm-ZoneVariance	0.007351685
original-ngtdm-Busyness	0.017242836
original-ngtdm-Complexity	6.96925E-09
original-ngtdm-Contrast	5.10917E-06
original-ngtdm-Strength	0.0010726

There are 13 significant differences between the enhanced lung window and the mediastinal window, as shown in Table 7.

According to pathological grouping testing, 54 cases were found to have significant differences between squamous cell carcinoma and adenocarcinoma, as shown in Table Table 8.

Table 6 significant differences between the lung window and mediastinal window in plain scan

characteristics	P
original-firstorder-10Percentile	2.82492E-06
original-firstorder-Energy	2.07957E-06
original-firstorder-Skewness	0.02714996
original-glcm-Idmn	0.02889707
original-gldm-DependenceVariance	0.013117159
original-glszm-SmallAreaHighGrayLevelEmphasis	1.55274E-05
original-glszm-SmallAreaLowGrayLevelEmphasis	0.000889334
original-glszm-ZoneEntropy	5.5166E-05
original-glszm-ZonePercentage	2.30186E-05
original-glszm-ZoneVariance	0.005005096
original-ngtdm-Busyness	0.000889334
original-ngtdm-Complexity	1.77955E-06
original-ngtdm-Contrast	5.5166E-05
original-ngtdm-Strength	7.88072E-05

Table 7 significant differences between the enhanced lung window and the mediastinal window

characteristics	P
original-firstorder-10Percentile	7.7589E-07
original-firstorder-Energy	6.80587E-06
original-glcm-Imc1	0.025492812
original-glrlm-LongRunHighGrayLevelEmphasis	0.030737842
original-glrlm-LowGrayLevelRunEmphasis	0.019692889
original-glszm-SmallAreaHighGrayLevelEmphasis	5.90131E-06
original-glszm-SmallAreaLowGrayLevelEmphasis	7.0054E-05
original-glszm-ZoneEntropy	5.10917E-06
original-glszm-ZonePercentage	0.000330363
original-ngtdm-Busyness	0.015058807
original-ngtdm-Complexity	1.62759E-07
original-ngtdm-Contrast	0.000156071
original-ngtdm-Strength	0.002194965

By sequentially plotting the above image features, it can be seen that groups 1 and 3 are more distinct. Considering that groups 1 and 3 have more advantages in distinguishing between squamous cell carcinoma and adenocarcinoma compared to groups 2 and 4 (Figs. 1, 2, 3, 4, 5 and 6).

Discussion

The incidence of lung cancer ranks second among malignant tumors, while the mortality rate ranks first [1]. In order to clarify the pathological properties [2–4, 21], gene status [5, 6], treatment efficacy [7, 8, 17, 22–24], recurrence risk [7, 8, 17, 22–24], survival time [11, 12, 25, 26], and distinguish radiation pneumonia [13, 14],

Table 8 significant differences between squamous cell carcinoma and adenocarcinoma

characteristics	P
original-shape-Elongation	0.013153277
original-shape-Flatness	0.034639767
original-shape-LeastAxisLength	3.11E-05
original-shape-MajorAxisLength	2.44E-05
original-shape-Maximum2DDiameterColumn	0.000134437
original-shape-Maximum2DDiameterRow	0.000377624
original-shape-Maximum2DDiameterSlice	1.22E-05
original-shape-Maximum3DDiameter	0.000269693
original-shape-MeshVolume	0.00107793
original-shape-MinorAxisLength	4.22E-06
original-shape-SurfaceArea	5.40E-05
original-shape-SurfaceVolumeRatio	0.008647681
original-shape-VoxelVolume	0.001118603
original-firstorder-Entropy	0.040893511
original-firstorder-InterquartileRange	0.007386044
original-firstorder-Kurtosis	0.001257898
original-firstorder-Range	0.040891333
original-firstorder-RobustMeanAbsoluteDeviation	0.036122056
original-firstorder-Skewness	0.000737878
original-firstorder-Uniformity	0.010562257
original-glcm-Idn	0.025077306
original-glcm-Imc1	0.047117091
original-glcm-Imc2	0.012533799
original-glcm-SumEntropy	0.023464294
original-gldm-DependenceEntropy	0.008868887
original-gldm-DependenceNonUniformity	0.00056928
original-gldm-GrayLevelNonUniformity	0.00056928
original-gldm-HighGrayLevelEmphasis	0.036122056
original-gldm-LowGrayLevelEmphasis	0.027976743
original-gldm-SmallDependenceLowGrayLevelEmphasis	0.014820466
original-glrlm-GrayLevelNonUniformity	0.000227723
original-glrlm-GrayLevelNonUniformityNormalized	0.00801305
original-glrlm-HighGrayLevelRunEmphasis	0.036122056
original-glrlm-LongRunHighGrayLevelEmphasis	0.014820466
original-glrlm-LowGrayLevelRunEmphasis	0.025635667
original-glrlm-RunLengthNonUniformity	0.001337266
original-glrlm-ShortRunHighGrayLevelEmphasis	0.040893511
original-glrlm-ShortRunLowGrayLevelEmphasis	0.021941184
original-glszm-GrayLevelNonUniformity	1.31E-05
original-glszm-HighGrayLevelZoneEmphasis	0.012533799
original-glszm-LargeAreaEmphasis	0.007810867
original-glszm-LargeAreaHighGrayLevelEmphasis	0.002220192
original-glszm-LargeAreaLowGrayLevelEmphasis	0.017462591
original-glszm-LowGrayLevelZoneEmphasis	0.009562788
original-glszm-SizeZoneNonUniformity	5.00E-05
original-glszm-SizeZoneNonUniformityNormalized	9.20E-05
original-glszm-SmallAreaEmphasis	8.86E-05
original-glszm-SmallAreaHighGrayLevelEmphasis	0.004738257
original-glszm-SmallAreaLowGrayLevelEmphasis	0.039247488
original-glszm-ZoneVariance	0.007613218
original-ngtdm-Busyness	5.61E-05
original-ngtdm-Coarseness	1.62E-05
original-ngtdm-Complexity	0.041737989
original-ngtdm-Strength	0.003312745

significant progress has been made in research on imaging features. In recent years, most researchers have chosen the radiomics component of 3D-Slicer software for image feature extraction due to its simple operability [15], but its application lacks standardization. Differences in positioning, acquisition, and segmentation, differences in contrast agents, image quality issues, and exclusion of patients with T4 lesions due to the uncertainty of lesion examination and potential bias in the final results.

Some studies use non enhanced CT to extract image features [7, 10, 11, 17, 26–28]. some studies use enhanced CT to extract image features [5, 6, 8, 9, 12, 29–31], some studies are uncertain whether to apply enhanced CT [22], some studies apply PET-CT [32–34]. However, Stefano conducted a comprehensive search and found that applying PET-CT for image segmentation has poor stability [16], so we chose CT images for our research. Tamponi analyzed the effect of enhancers on the extraction of omics features in a total of 17 patients, with GTV as tumor. Segmentation was performed by two hospitalized radiologists or radiation oncologists, and then revised by two radiologists. It was found that contrast agents have a significant impact, affecting approximately 90% of features [35]. No further relevant research has been found. At present, the extraction of imaging features in radiomics mostly uses the selection of lung window to delineate the tumor range, or the expansion of a certain boundary of the lung window tumor range to analyze tumor infiltration and treatment response. A few choose to delineate the mediastinal window or do not have a clear expression. At present, there is no clear article recommending the use of enhanced CT or plain CT when extracting imaging omics, nor is there clear data support. The aim of this study is to conduct a preliminary analysis of the enhancement effect of CT and the differences in the selection of lung or mediastinal windows, in order to understand their impact on image feature extraction. I hope to provide a basis for future image feature extraction. In addition, many articles have proposed that radiomics is of great significance in the pathological differentiation of adenocarcinoma and squamous cell carcinoma [2–4]. Some research found that radiomics

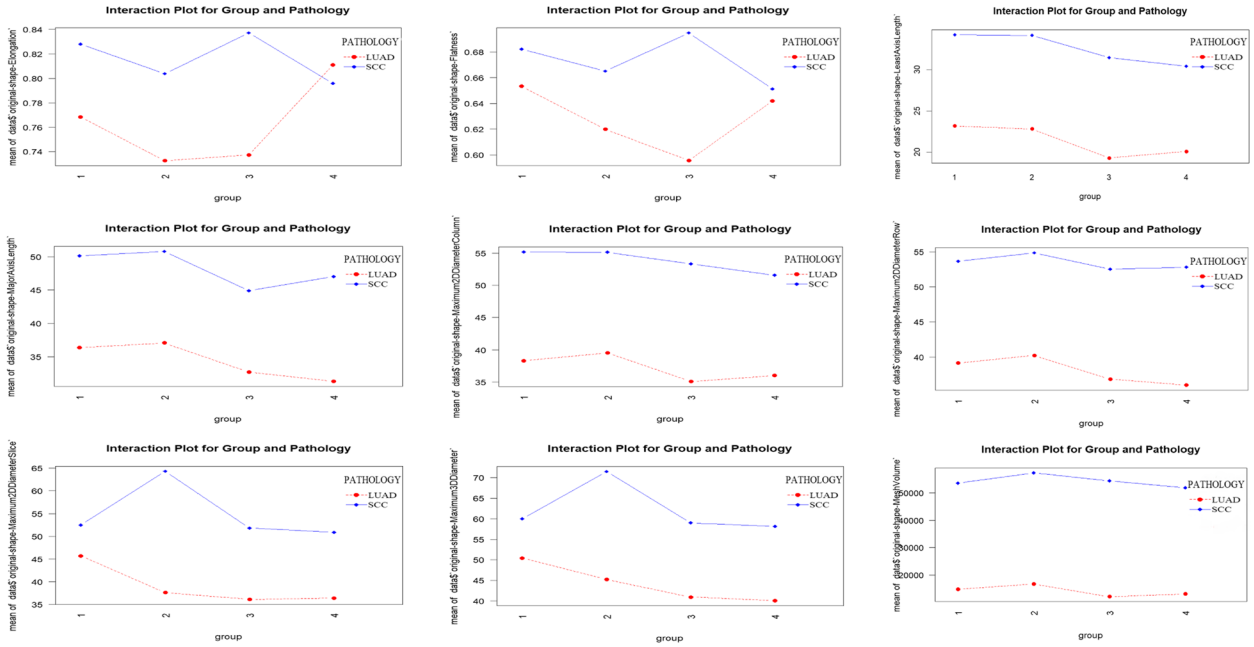

Fig. 1 Diagram of image features for each group

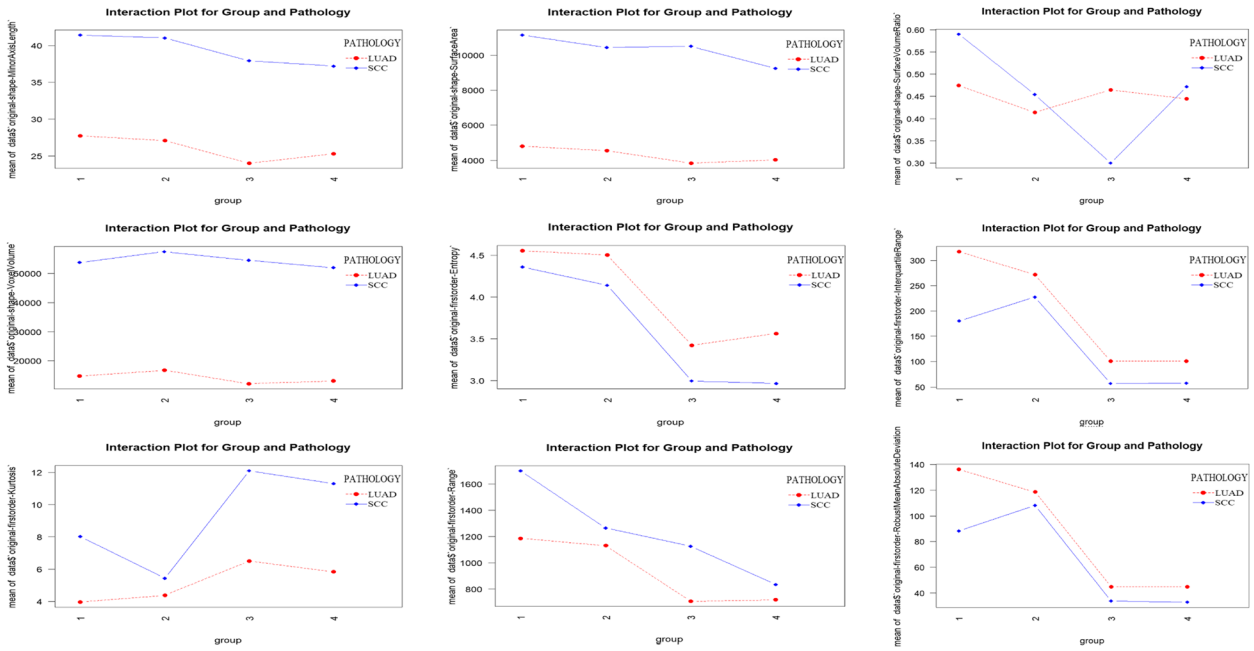

Fig. 2 Diagram of image features for each group

features can effectively distinguish between lung squamous cell carcinoma and lung adenocarcinoma [21, 36], but the impact of CT image enhancement and target delineation in the lung or mediastinal window is not clear in these study. Garau found that the imaging radiomics of plain CT can effectively distinguish between benign and malignant pulmonary nodules, and attempted to apply Combat harmonization method to reduce the influence of different brands of CT and scan parameters, but found no significant differences [37].

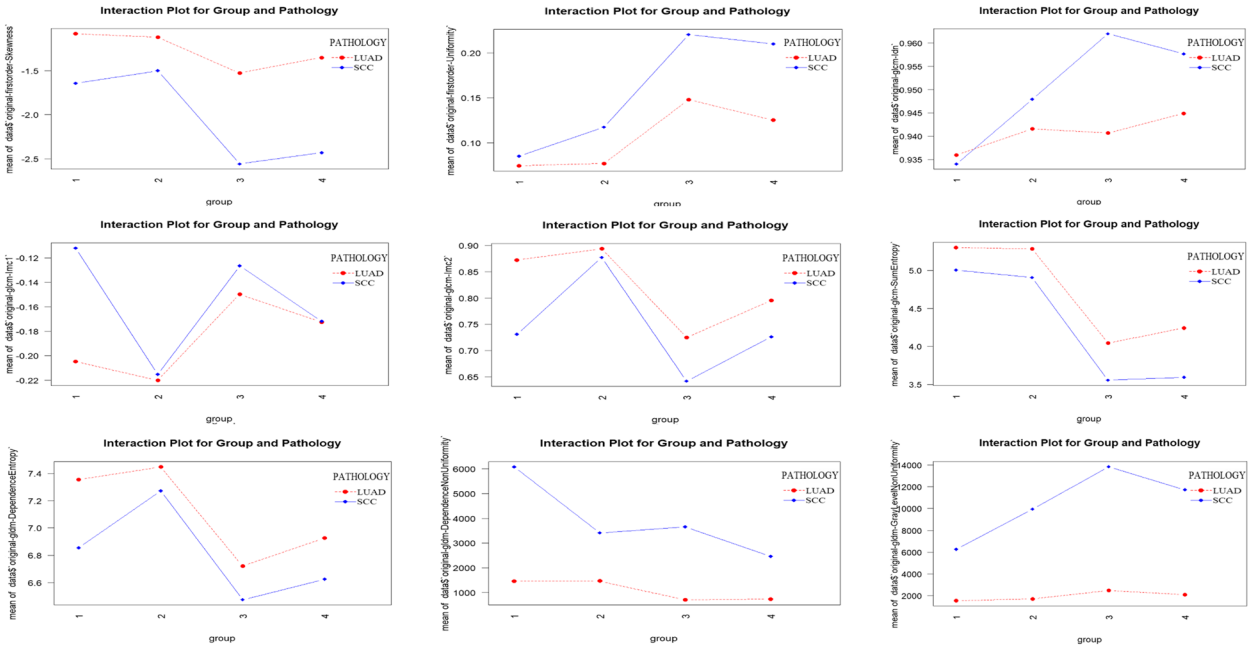

Fig. 3 Diagram of image features for each group

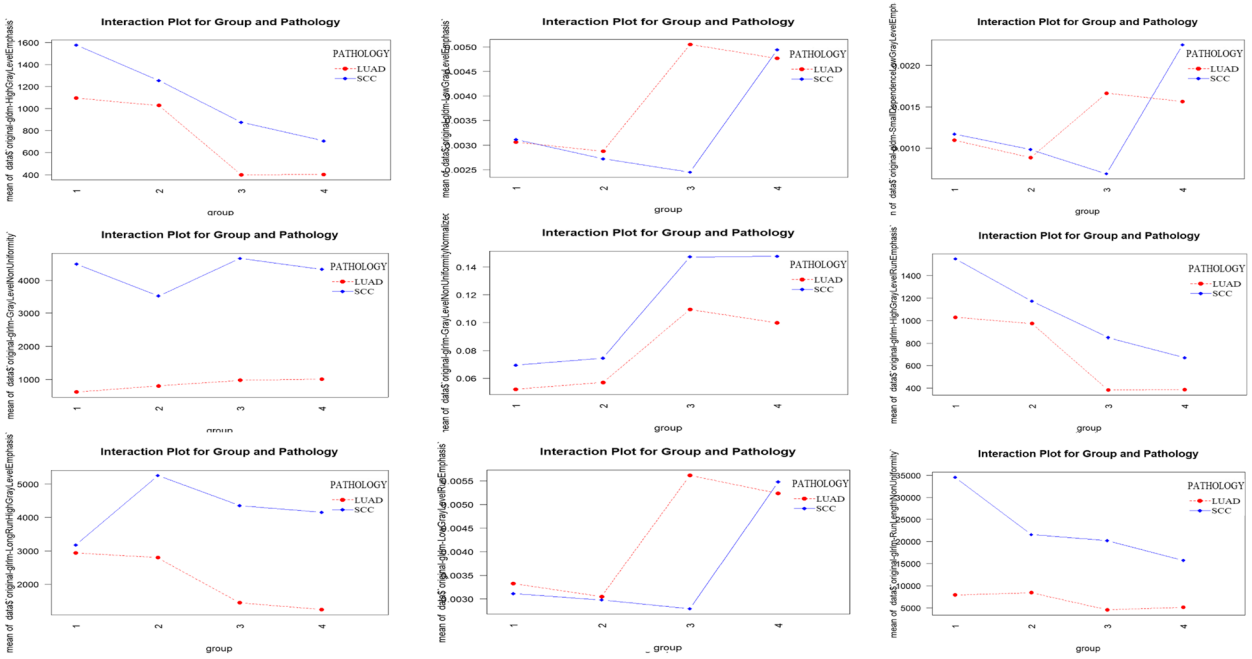

Fig. 4 Diagram of image features for each group

This article briefly analyzes the differences in the impact of imaging radiomics features on lung squamous cell carcinoma and adenocarcinoma under different combinations of enhanced CT or plain CT, lung window or mediastinal window conditions. Four sets of influencing features were extracted for each patient, namely the plain lung window group, plain mediastinal window group, enhanced lung window group, and enhanced mediastinal window group. A total of 88 sets of image features were extracted, each containing 851

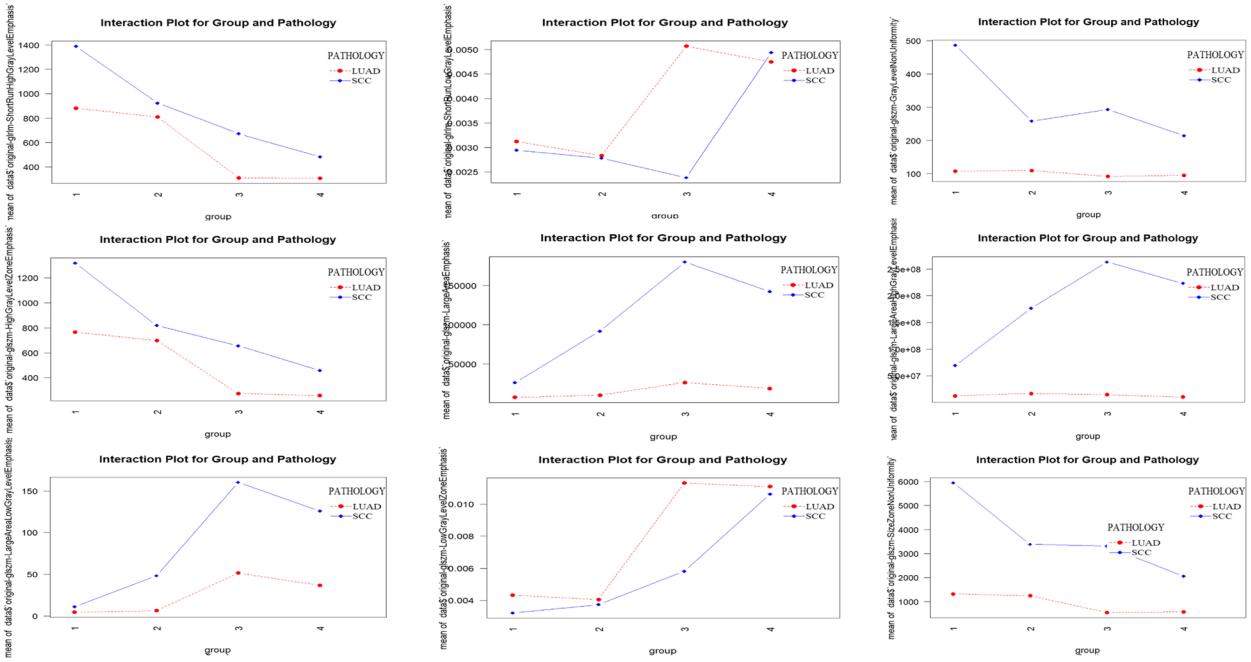

Fig. 5 Diagram of image features for each group

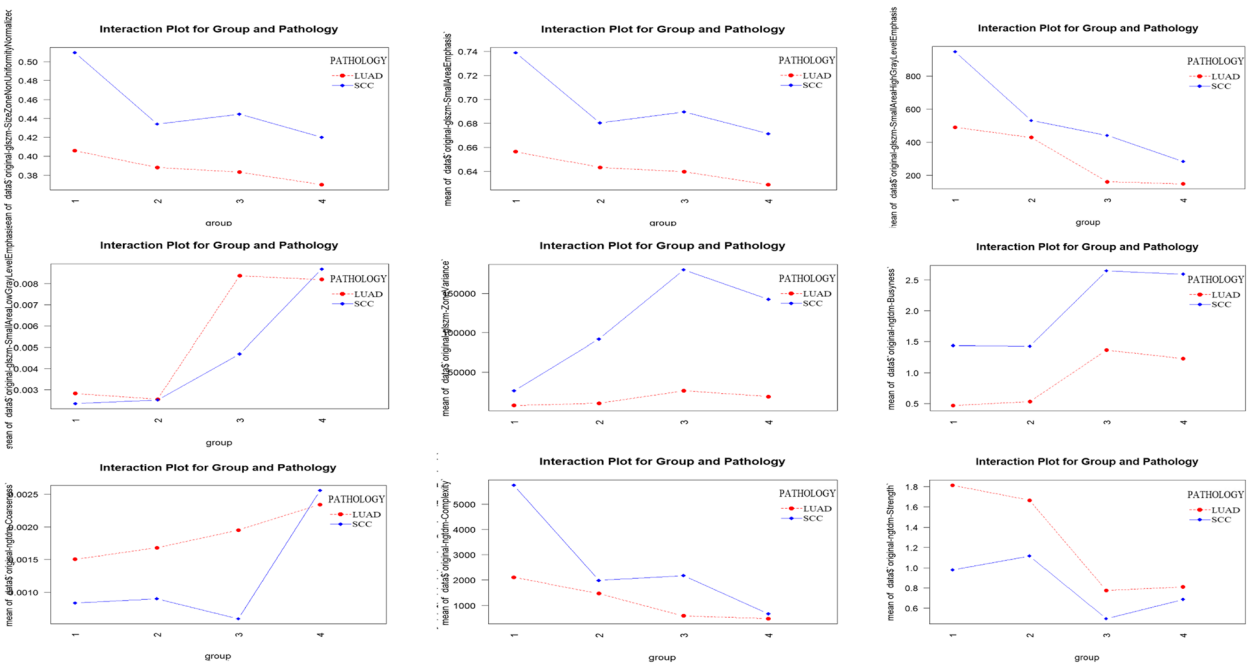

Fig. 6 Diagram of image features for each group

features. Due to filtering adjustments made to sequences outside the original sequence, the stability cannot be determined. Therefore, a total of 107 features of the original sequence were selected for analysis. Four sets of data for each feature were first subjected to Shapiro tests, all of which were non normal distributions, and Friedman tests were performed. Among them, 33 features showed significant differences. Continuing with pairwise repeated detection, it was found that there were 2 significant differences between

enhanced and nonenhanced lung windows, namely origin glcm Imc1 and origin ngtdm Complexity, indicating a significant difference in the amplitude of image changes. This may be due to the enhancement of adjacent pixel differences in enhanced CT. There are 12 imaging features that show significant differences between the enhanced lung window and the plain scanning mediastinal window, indicating a significant difference in grayscale between the two, especially in the 10th percentile, and there is also a significant difference in adjacent grayscale differences. The plain scanning mediastinal window and the plain scanning mediastinal window show a significant difference in grayscale, with 1 being the original firster-90 percentile, indicating a significant difference in grayscale between the 90th percentile. There are 14 significant differences between the plain scanning lung window and the enhanced mediastinal window group, indicating a significant difference in grayscale between the two, especially in the 10th percentile, and there is also a significant difference in adjacent grayscale differences, as well as a significant difference in the size of low-intensity grayscale areas. There are 14 imaging features with significant differences between the lung window and mediastinal window in plain scan, indicating a significant difference in grayscale between the two, especially in the 10th percentile, and there are also significant differences in adjacent grayscale differences. There are 13 imaging features with significant differences between the enhanced lung window and the mediastinal window, indicating a significant difference in grayscale between the two, especially in the 10th percentile. There are also significant differences in adjacent grayscale differences, with significant differences in large areas of homogeneous high grayscale areas and significant differences in homogeneous low grayscale areas. Different from our guess, image segmentation is carried out according to different conditions of lung window and mediastinum window. We originally thought that there would be significant differences in shape, but the result is that there are significant differences in gray level differences, which may be different from the lung window image segmentation, which includes a large number of tumor edge areas, and the gray level differences in tumor edge areas change more than the changes in tumor interior. The application of enhanced CT also affects the grayscale of lung window image segmentation, but the affected features are only two, and the grayscale impact on mediastinal window image segmentation is even more limited. Then, based on pathology, the data were divided into two groups: 44 groups of 11 squamous cell carcinoma patients and 44 groups of 11 adenocarcinoma patients, which displayed abnormal distribution. Wilcoxon's rank test was performed, and 54 imaging features were found to have significant differences between squamous cell carcinoma and adenocarcinoma, accounting for more than half of the original sequence By sequentially plotting the above image features, it can be seen that groups 1 and 3 have more advantages in distinguishing between squamous cell carcinoma and adenocarcinoma compared to groups 2 and 4, that is, extracting image features from plain CT may be better than enhancing CT. Liu found that the enhanced features of CT are not the main imaging features for distinguishing squamous cell carcinoma from adenocarcinoma, which is consistent with the conclusion of this study [38]. Image segmentation and image feature extraction are the cornerstone of imaging omics research. For the selection of plain CT or enhanced CT, as well as the selection of lung window or mediastinal window for image segmentation, this article provides a basis for image selection and segmentation in image feature research, reduces possible biases in image feature extraction data, and contributes to the homogenization progress of future image feature extraction. However, this study also has certain limitations, the CT images included in the study have different hospitals, brands, batches, and scan parameters, which may affect research conclusions, despite undergoing resampled image preprocessing method [21]. But there is currently no clear and effective method to avoid such impacts [39, 40]. In addition, the small number of patients included in this study may have a biased impact on the research results. And Image segmentation is carried out from the mediastinal window and the lung window, and amount of radiomics data with significant differences are extracted, which are quite important. However, whether these data will affect differential diagnosis and prognosis still requires further investigation. In the future, we will establish models for differential diagnosis and prognosis prediction and make comparisons to evaluate the impact of the lung window and the mediastinal window on the prediction models. Meanwhile, in future studies, we will expand the patient population to obtain more convincing results.

Conclusions

The enhancement of lung CT has a relatively small impact on extracting image features, and the selection of lung or mediastinal windows during image segmentation has a greater impact on the grayscale changes in extracting image features. Therefore, the selection of lung or mediastinal windows for feature extraction should be carefully considered. The size of the image segmentation range has a greater impact on image features, indicating

that the tumor edge area contains richer changes in image features. The impact of lung squamous cell carcinoma and adenocarcinoma on imaging features is also significant, indicating a high possibility of distinguishing between squamous cell carcinoma and adenocarcinoma based on radiomics.

Supplementary Information

The online version contains supplementary material available at https://doi.org/10.1186/s12885-025-14094-z.

Supplementary Material 1.

Authors' contributions

Chunmei Liu wrote the manuscript and all the figures, downloaded imaging and applying 3DSLICER for Image Segmentation and Feature Extraction, Yuzheng He jointly applied 3DSLICER for Image Segmentation and Feature Extraction, Jianmin Luo design the study. All authors gone over and ratified the ultimate manuscript.

Funding

This work was supported by the Health of Hebei Province Commission for medical scientific research funding of China (No. 20180396).

Data availability

No datasets were generated or analysed during the current study.

Declarations

Ethics declarations and consent to participate

The study was approved by the Research Ethics Committee of the second hospital of Hebei Medical University (approval no 2024-R019) and was conducted in accordance with the 1964 Helsinki Declaration and its later amendments or comparable ethical standards. This study is based on publicly available data for analysis, all of which have been anonymized and cannot identify specific individuals. Therefore, no informed consent is required.

Consent for publication

Not applicable.

Competing interests

The authors declare no competing interests.

Author details

[1]Department of Radiation Oncology, The Second Hospital of Hebei Medical University, 215 West Heping Road, Shijiazhuang, Hebei Province, China. [2]Department of Thoracic Surgery, The Second Hospital of Hebei Medical University, 215 West Heping Road, Shijiazhuang, Hebei Province, China. [3]Department of Hematology, The Second Hospital of Hebei Medical University, 215 West Heping Road, Shijiazhuang, Hebei Province, China.

Received: 14 May 2024 Accepted: 6 April 2025
Published online: 17 April 2025

References

1. Bade BC, Dela Cruz CS. Lung Cancer 2020: Epidemiology, Etiology, and Prevention. Clin Chest Med. 2020;41(1):1–24.
2. Tomori Y, Yamashiro T, Tomita H, Tsubakimoto M, Ishigami K, Atsumi E, et al. CT radiomics analysis of lung cancers: Differentiation of squamous cel l carcinoma from adenocarcinoma, a correlative study with FDG uptake. Eur J Radiol. 2020;128:109032.
3. Lin J, Yu Y, Zhang X, Wang Z, Li S**.** Classification of Histological Types and Stages in Non-small Cell Lung Cancer Using Radiomic Features Based on CT Images. J Dig Imag. 2023;36(3):1029–37.
4. Tang X, Huang H, Du P, Wang L, Yin H, Xu X**.** Intratumoral and peritumoral CT-based radiomics strategy reveals disti nct subtypes of non-small-cell lung cancer. J Cancer Res Clin Oncol. 2022;148(9):2247–60.
5. He R, Yang X, Li T, He Y, Xie X, Chen Q, et al. A Machine Learning-Based Predictive Model of Epidermal Growth Factor Mutations in Lung Adenocarcinomas. Cancers (Basel). 2022;14(19):4664.
6. Wu S, Shen G, Mao J, Gao B. CT Radiomics in Predicting EGFR Mutation in Non-small Cell Lung Cancer: A Single Institutional Study. Front Oncol. 2020;10: 542957.
7. Wang J, Wang J, Huang X, Zhou Y, Qi J, Sun X, et al. CT radiomics-based model for predicting TMB and immunotherapy response in non-small cell lung cancer. BMC Med Imaging. 2024;24(1):45.
8. Khorrami M, Prasanna P, Gupta A, Patil P, Velu PD, Thawani R, et al. Changes in CT Radiomic Features Associated with Lymphocyte Distribution Predict Overall Survival and Response to Immunotherapy in Non-Small Cell Lung Cancer. Cancer Immunol Res. 2020;8(1):108–19.
9. Akinci D'Antonoli T, Farchione A, Lenkowicz J, Chiappetta M, Cicchetti G, Martino A, et al. CT Radiomics Signature of Tumor and Peritumoral Lung Parenchyma to Predict Nonsmall Cell Lung Cancer Postsurgical Recurrence Risk. Acad Radiol. 2020;27(4):497–507.
10. Davey A, van Herk M, Faivre-Finn C, Brown S, McWilliam A**.** Optimising use of 4D-CT phase information for radiomics analysis in lung cancer patients treated with stereotactic body radiotherapy. Phys Med Biol. 2021;66(11):115012.
11. Pérez-Morales J, Tunali I, Stringfield O, Eschrich SA, Balagurunathan Y, Gillies RJ, et al. Peritumoral and intratumoral radiomic features predict survival outcomes among patients diagnosed in lung cancer screening. Sci Rep. 2020;10(1):10528.
12. Tunali I, Stringfield O, Guvenis A, Wang H, Liu Y, Balagurunathan Y, et al. Radial gradient and radial deviation radiomic features from pre-surgical CT scans are associated with survival among lung adenocarcinoma patients. Oncotarget. 2017;8(56):96013–26.
13. Qiu Q, Xing L, Wang Y, Feng A, Wen Q**.** Development and Validation of a Radiomics Nomogram Using Computed Tomography for Differentiating Immune Checkpoint Inhibitor-Related Pneumonitis From Radiation Pneumonitis for Patients With Non-Small Cell Lung Cancer. Front Immunol. 2022;13:870842.
14. Kong Y, Su M, Zhu Y, Li X, Zhang J, Gu W, et al. Enhancing the prediction of symptomatic radiation pneumonitis for locally advanced non-small-cell lung cancer by combining 3D deep learning-derived imaging features with dose-volume metrics: a two-center study. Strahlenther Onkol. 2024.
15. van Griethuysen JJM, Fedorov A, Parmar C, Hosny A, Aucoin N, Narayan V, Beets-Tan RGH, Fillon-Robin JC, Pieper S, Aerts HJWL. Computational Radiomics System to Decode the Radiographic Phenotype. Can Res. 2017;77(21):e104–7.
16. Stefano A. Challenges and limitations in applying radiomics to PET imaging: Possible opportunities and avenues for research. Comput Biol Med. 2024;179: 108827.
17. Khorrami M, Khunger M, Zagouras A, Patil P, Thawani R, Bera K, et al. Combination of Peri- and Intratumoral Radiomic Features on Baseline CT Scans Predicts Response to Chemotherapy in Lung Adenocarcinoma. Radiol Artif Intell. 2019;1(2): e180012.
18. Liu C, He Y, Luo J. The Influence of Image Selection and Segmentation on the Extraction of Lung Cancer Imaging Radiomics Features Using 3D-Slicer Software. Abstract Book of MEDLIFE2024 & IC`BLS2024.; 2024.
19. National Cancer Institute Clinical Proteomic Tumor Analysis Consortium (CPTAC). The Clinical Proteomic Tumor Analysis Consortium Lung Squamous Cell Carcinoma Collection (CPTAC-LSCC) (Version 14). The Cancer Imaging Archive. 2018. https://doi.org/10.7937/K9/TCIA.2018.6EMUB5L2.
20. Albertina B, Watson M, Holback C, Jarosz R, Kirk S, Lee Y, Rieger-Christ K, Lemmerman J. The Cancer Genome Atlas Lung Adenocarcinoma Collection (TCGA-LUAD) (Version 4). The Cancer Imaging Archive. 2016. https://doi.org/10.7937/K9/TCIA.2016.JGNIHEP5.
21. Pasini G, Stefano A, Russo G, Comelli A, Marinozzi F, Bini F**.** Phenotyping the Histopathological Subtypes of Non-Small-Cell Lung Carcinoma: How Beneficial Is Radiomics? Diagn (Basel). 2023;13(6):1167.
22. Vaidya P, Bera K, Gupta A, Wang X, Corredor G, Fu P, et al. CT derived radiomic score for predicting the added benefit of adjuvant chemotherapy following surgery in stage I, II resectable non-small cell lung cancer: a retrospective multicohort study for outcome prediction. Lancet Digit Health. 2020;2(3):e116–28.

23. Khorrami M, Jain P, Bera K, Alilou M, Thawani R, Patil P, et al. Predicting pathologic response to neoadjuvant chemoradiation in resectable stage III non-small cell lung cancer patients using computed tomography radiomic features. Lung Cancer. 2019;135:1–9.
24. de Miguel-Perez D, Ak M, Mamindla P, Russo A, Zenkin S, Ak N, et al. Validation of a multiomic model of plasma extracellular vesicle PD-L1 and radiomics for prediction of response to immunotherapy in NSCLC. J Exp Clin Cancer Res. 2024;43(1):81.
25. Hou KY, Chen JR, Wang YC, Chiu MH, Lin SP, Mo YH, et al. Radiomics-Based Deep Learning Prediction of Overall Survival in Non-Small-Cell Lung Cancer Using Contrast-Enhanced Computed Tomography. Cancers (Basel). 2022;14(15):3798.
26. D'Amico NC, Sicilia R, Cordelli E, Tronchin L, Soda P. Radiomics-Based Prediction of Overall Survival in Lung Cancer Using Different Volumes-Of-Interest. Appl Sci. 2020;10(18):6425.
27. Wang T, She Y, Yang Y, Liu X, Chen S, Zhong Y, et al. Radiomics for Survival Risk Stratification of Clinical and Pathologic Stage IA Pure-Solid Non-Small Cell Lung Cancer. Radiology. 2022;302(2):425–34.
28. Xu F, Zhu W, Shen Y, Wang J, Xu R, Qutesh C, et al. Radiomic-Based Quantitative CT Analysis of Pure Ground-Glass Nodules to Predict the Invasiveness of Lung Adenocarcinoma. Front Oncol. 2020;10:872.
29. Liu K, Li K, Wu T, Liang M, Zhong Y, Yu X, et al. Improving the accuracy of prognosis for clinical stage I solid lung adenocarcinoma by radiomics models covering tumor per se and peritumoral changes on CT. Eur Radiol. 2022;32(2):1065–77.
30. Dou TH, Coroller TP, van Griethuysen JJM, Mak RH, Aerts H. Peritumoral radiomics features predict distant metastasis in locally advanced NSCLC. PLoS ONE. 2018;13(11): e0206108.
31. Owens CA, Peterson CB, Tang C, Koay EJ, Yu W, Mackin DS, et al. Lung tumor segmentation methods: Impact on the uncertainty of radiomics features for non-small cell lung cancer. PLoS ONE. 2018;13(10): e0205003.
32. Bogowicz M, Vuong D, Huellner MW, Pavic M, Andratschke N, Gabrys HS, et al. CT radiomics and PET radiomics: ready for clinical implementation? Q J Nucl Med Mol Imaging. 2019;63(4):355–70.
33. Tong H, Sun J, Fang J, Zhang M, Liu H, Xia R, et al. A Machine Learning Model Based on PET/CT Radiomics and Clinical Characteristics Predicts Tumor Immune Profiles in Non-Small Cell Lung Cancer: A Retrospective Multicohort Study. Front Immunol. 2022;13: 859323.
34. Ma N, Yang W, Wang Q, Cui C, Hu Y, Wu Z. Predictive value of (18)F-FDG PET/CT radiomics for EGFR mutation status in non-small cell lung cancer: a systematic review and meta-analysis. Front Oncol. 2024;14:1281572.
35. Tamponi M, Crivelli P, Montella R, Sanna F, Gabriele D, Poggiu A, et al. Exploring the variability of radiomic features of lung cancer lesions on unenhanced and contrast-enhanced chest CT imaging. Phys Med. 2021;82:321–31.
36. Song F, Song X, Feng Y, Fan G, Sun Y, Zhang P, et al. Radiomics feature analysis and model research for predicting histopathological subtypes of non-small cell lung cancer on CT images: A multi-dataset study. Med Phys. 2023;50(7):4351–65.
37. Garau N, Paganelli C, Summers P, Choi W, Alam S, Lu W, et al. External validation of radiomics-based predictive models in low-dose CT screening for early lung cancer diagnosis. Med Phys. 2020;47(9):4125–36.
38. Liu C, He Y, Luo J**.** Application of Chest CT Imaging Feature Model in Distinguishing Squamo us Cell Carcinoma and Adenocarcinoma of the Lung. Cancer Manage Res. 2024;16:547–57.
39. Mali SA, Ibrahim A, Woodruff HC, Andrearczyk V, Müller H, Primakov S, et al. Making Radiomics More Reproducible across Scanner and Imaging Protocol Variations: A Review of Harmonization Methods. J Pers Med. 2021;11(9):842.
40. Da-Ano R, Visvikis D, Hatt M**.** Harmonization strategies for multicenter radiomics investigations. Phys Med Biol. 2020;65(24):24tr02.

Publisher's Note